A Tetranuclear Ruthenium(II) Complex Containing both Electron-Rich and Electron-Poor Bridging Ligands. Absorption Spectrum, Luminescence, Redox Behavior, and Intercomponent Energy Transfer

Scolastica Serroni,[1a] Sebastiano Campagna,*[,1a] Gianfranco Denti,[1b] Tia E. Keyes,[1c] and Johannes G. Vos*[,1c]

Dipartimento di Chimica Inorganica, Analitica e Struttura Molecolare dell'Università, via Sperone 31, I-98166 Vill. S. Agata, Messina, Italy, Laboratorio di Chimica Inorganica, Istituto di Chimica Agraria dell'Università, via S. Michele degli Scalzi 2, I-50124 Pisa, Italy, and School of Chemical Sciences, Dublin City University, Dublin 9, Ireland

Received January 26, 1995[⊗]

The first luminescent and redox active multinuclear Ru(II) compound containing *both* electron-poor (2,3-bis(2-pyridyl)pyrazine, 2,3-dpp) and electron-rich (3,5-bis(pyridyn-2-yl)-1,2,4-triazole, Hbpt) polypyridine bridging ligands has been synthesized. The novel compound is $[(bpy)_2Ru(\mu\text{-bpt})Ru\{(\mu\text{-2,3-dpp})Ru(bpy)_2\}_2]^{7+}$ (**1**; bpy = 2,2′-bipyridine). Its absorption spectrum, luminescence properties, and redox behavior have been studied and are compared with the properties of the parent complexes $[Ru\{(\mu\text{-2,3-dpp})Ru(bpy)_2\}_3]^{8+}$ (**2**) and $[(bpy)_2Ru(\mu\text{-bpt})Ru(bpy)_2]^{3+}$ (**3**). The absorption spectrum of **1** is dominated by ligand-centered bands in the UV region and by metal-to-ligand charge transfer bands in the visible region. Excited states and oxidation and reduction processes are localized in specific sites of the multicomponent structure. However, perturbations of each component on the redox and excited states of the others, as well as electronic interactions between the chromophores, can be observed. Intercomponent energy transfer from the upper-lying $(\mu\text{-bpt})(bpy)Ru\rightarrow bpy$ CT excited state of the $Ru(bpy)_2(\mu\text{-bpt})^+$ component to the lower-lying $(bpy)_2Ru\rightarrow\mu\text{-2,3-dpp}$ CT excited state of the $Ru(bpy)_2(\mu-2,3\text{-dpp})^{2+}$ subunit(s) is efficient in **1** in fluid solution at room temperature, whereas this process is not observed in a rigid matrix at 77 K. A two-step energy transfer mechanism is proposed to explain the photophysical properties of the new compound.

Introduction

Luminescent and redox-active multinuclear metal complexes are currently the object of great interest because of both theoretical reasons and potential practical applications. For example, this family of compounds holds a central position in the design of supramolecular systems capable of performing photoinduced energy migration and/or charge separation, with the ultimate goal of constructing devices for solar energy conversion and/or light-driven information processing.[2]

A major class of luminescent and redox-active multinuclear metal complexes is based on Ru(II)−polypyridine building blocks connected by electron-poor (i.e., with low-lying π^* orbitals) bridging ligands. One of the most used bridging ligand is the bis-chelating ligand 2,3-bis(2-pyridyl)pyrazine (2,3-dpp).[3,4] A second class of luminescent multinuclear metal complexes is based on the same building blocks connected by anionic electron-rich (with relatively high-lying π orbitals) bridging ligands.[5−8] An interesting difference between the two classes of multinuclear systems is that electron-poor bridging ligands can mediate metal−metal communication by a superexchange

⊗ Abstract published in *Advance ACS Abstracts,* May 15, 1996.

(1) (a) Università di Messina. (b) Università di Pisa. (c) Dublin City University.

(2) (a) Meyer, T. J. *Acc. Chem. Res.* **1989**, *22*, 163. (b) Scandola, F.; Indelli, M. T.; Chiorboli, C.; Bignozzi, C. A. *Top. Curr. Chem.* **1990**, *158*, 73. (c) Balzani, V.; Scandola, F. *Supramolecular Photochemistry*; Horwood: Chichester, U.K., 1991. (d) Jones, W. E.; Baxter, S. M.; Mecklenburg, S. L.; Erickson, B. W.; Peek, B. M.; Meyer, T. J. In *Supramolecular Chemistry*; Balzani, V., De Cola, L., Eds.; Kluwer: Dordrecht, The Netherlands, 1992; p 249. (e) Denti, G.; Serroni, S.; Campagna, S.; Juris, A.; Ciano, M.; Balzani, V. In *Perspectives in Coordination Chemistry*; Williams, A. F.; Floriani, C.; Merbach, A. E., Eds.; VCH: Basel, 1992, p 153. (f) Amadelli, R.; Argazzi, R.; Bignozzi, C. A.; Scandola, F. *J. Am. Chem. Soc.* **1990**, *112*, 7099. (g) O'Regan, B.; Graetzel, M. *Nature* **1991**, *353*, 737. (h) Vögtle, F.; Frank, M.; Nieger, M.; Belser, P.; von Zelewsky, A.; Balzani, V.; Barigelletti, F.; De Cola, L.; Flamigni, L. *Angew. Chem., Int. Ed. Engl.* **1993**, *32*, 1643. (i) Barigelletti, F.; Flamigni, L.; Balzani, V.; Collin, J.-P.; Sauvage, J.-P.; Sour, A.; Constable, E. C.; Cargill Thompson, A. M. W. *J. Am. Chem. Soc.* **1994**, *116*, 7692. (j) Collin, J.-P.; Harriman, A.; Heitz, V.; Odobel, F.; Sauvage, J.-P. *J. Am. Chem. Soc.* **1994**, *116*, 5679. (k) Balzani, V.; Scandola, F. In *Comprehensive Supramolecular Chemistry*; Reinhoudt, D. N., Ed.; Pergamon Press: Oxford, England, in press.

(3) (a) Fuchs, Y.; Lofters, S.; Dieter, T.; Shi, W.; Morgan, R.; Strekas, T. C.; Gafney, H. D.; Backer, A. D. *J. Am. Chem. Soc.* **1987**, *109*, 269. (b) Murphy, W. R., Jr.; Brewer, K. J.; Gettliffe, G.; Petersen, J. D.; *Inorg. Chem.* **1989**, *28*, 81. (c) Akashek, T. S.; Jibril, I.; Shraim, A. *Inorg. Chim. Acta* **1990**, *175*, 171. (d) Cooper, J. B.; MacQueen, D. B.; Petersen, J. D.; Wertz, D. W. *Inorg. Chem.* **1990**, *29*, 3701. (e) Kalyanasundaram, K.; Graetzel, M.; Nazeeruddin, Md. K. *J. Phys. Chem.* **1992**, *96* , 5865. (f) Richter, M. M.; Brewer, K. J. *Inorg. Chem.* **1993**, *32*, 2827. (g) Johnson, J. E. B.; Ruminski, R. R. *Inorg. Chim. Acta* **1993**, *208*, 179.

(4) (a) Denti, G.; Campagna, S.; Sabatino, L.; Serroni, S.; Ciano, M.; Balzani, V. *Inorg. Chem.* **1990**, *29*, 4750; (b) Campagna, S.; Denti, G.; Serroni, S.; Ciano, M.; Balzani, V. *Inorg. Chem.* **1991**, *30*, 3728. (c) Denti, G.; Campagna, S.; Serroni, S.; Ciano, M.; Balzani, V. *J. Am. Chem. Soc.* **1992**, *114*, 2944. (d) Serroni, S.; Denti, G.; Campagna, S.; Juris, A.; Ciano, M.; Balzani, V. *Angew. Chem., Int. Ed. Engl.* **1992**, *31*, 1493. (e) Juris, A.; Balzani, V.; Campagna, S.; Denti, G.; Serroni, S.; Frei, G.; Güdel, H. U. *Inorg. Chem.* **1994**, *33*, 1491, and references therein. (f) Campagna, S.; Giannetto, A.; Serroni, S.; Denti, G.; Trusso, S.; Mallamace, F.; Micali, N. *J. Am. Chem. Soc.* **1995**, *117*, 1754. (g) Campagna, S.; Denti, G.; Serroni, S.; Juris, A.; Venturi, M.; Ricevuto, V.; Balzani, V. *Chem. Eur. J.* **1995**, *1*, 211.

(5) (a) Bignozzi, C. A.; Roffia, S.; Scandola, F. *J. Am. Chem. Soc.* **1985**, *107*, 1644. (b) Bignozzi, C. A.; Roffia, S.; Chiorboli, C.; Davila, J.; Indelli, M. T.; Scandola, F. *Inorg. Chem.* **1989**, *28*, 4350. (c) Bignozzi, C. A.; Bortolini, O.; Chiorboli, C.; Indelli, M. T.; Rampi, M. A.; Scandola, F. *Inorg. Chem.* **1992**, *31*, 172. (d) Bignozzi, C. A.; Argazzi, R.; Schoonover, J. R.; Gordon, K. C.; Dyer, B. R.; Scandola, F. *Inorg. Chem.* **1992**, *31*, 5260. (e) Bignozzi, C. A.; Argazzi, R.; Indelli, M. T.; Scandola, F. *Sol. Energy Mater. Sol. Cells* **1994**, *32*, 229. (f) Indelli, M. T.; Bignozzi, C. A.; Harriman, A.; Schoonover, J. R.; Scandola, F. *J. Am. Chem. Soc.* **1994**, *116*, 3768.

S0020-1669(95)00086-3 CCC: $12.00

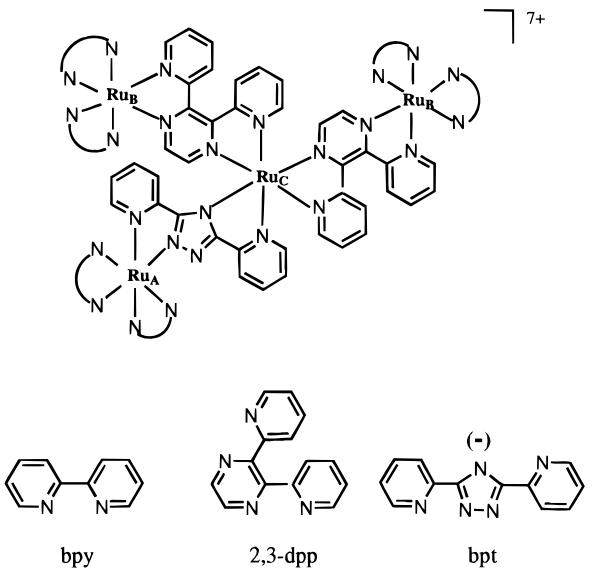

Figure 1. Structural formulas of the polypyridine ligands and schematic representation of **1** (N⁀N stands for bpy). The Ru metals are labeled as in the text.

mechanism essentially based on low-lying, empy π^* orbitals of the bridge (electron-transfer pathway), while electron-rich bridges may take advantage of relatively high-lying, full π orbitals (hole-transfer pathway).[9]

Here we report the synthesis and the photophysical and electrochemical properties of the first luminescent and redox-active multinuclear Ru(II) system in which *both* electron-poor (2,3-dpp) and electron-rich (3,5-bis(pyridin-2-yl)-1,2,4-triazolate, bpt) polypyridine bridges are present. The formula of the compound is $[(bpy)_2Ru(\mu\text{-bpt})Ru\{(\mu\text{-2,3-dpp})Ru(bpy)_2\}_2]^{7+}$ (**1**; bpy = 2,2′-bipyridine; for the structural formulas of the ligands, see Figure 1, in which a schematic representation of **1** is also given). Comparison with the properties of the parent complexes $[Ru\{(\mu\text{-2,3-dpp})Ru(bpy)_2\}_3]^{8+}$ (**2**) and $[(bpy)_2Ru(\mu\text{-bpt})Ru(bpy)_2]^{3+}$ (**3**) has also been made.

Experimental Section

Materials and Methods. $[Ru(bpy_2(bpt)](PF_6)$,[8a] $[Cl_2Ru(\mu\text{-2,3-dpp})Ru(bpy)_2\}_2](PF_6)_4$,[4b] $[Ru\{(\mu\text{-2,3-dpp})Ru(bpy)_2\}_3](PF_6)_8$,[4a] and $[(bpy)_2Ru(\mu\text{-bpt})Ru(bpy)_2](PF_6)_3$[8b] were available from previous works. Details on equipment and procedure for spectroscopic, photophysical, and electrochemical and spectroelectrochemical experiments have been previously reported.[4a,g] All the solvents and chemicals used were of the best commercial grade.

Experimental errors in the reported data are as follows: absorption maxima, 2 nm; luminescence maxima, 5 nm; molar absorption coefficients, 10%; emission lifetimes, 10%; emission quantum yields, 20%; redox potentials, 20 mV.

Synthesis of $[(bpy)_2Ru(\mu\text{-bpt})Ru\{(\mu\text{-2,3-dpp})Ru(bpy)_2\}_2](PF_6)_7$ (1). The trinuclear *complex-ligand*[2e] $[Cl_2Ru(\mu\text{-2,3-dpp})Ru(bpy)_2\}_2](PF_6)_4$ (0.045 g, 0.021 mmol) was dissolved in ethanol 95% (3 mL) and this was treated with 0.0008 g, 0.045 mmol of $AgNO_3$ in methanol (3mL) at room temperature. The reaction mixture turned blue as the precipitate of AgCl formed. The solution was left stirring for 3 h. The *complex-metal*[2e] $[Ru(bpy_2(bpt)](PF_6)$ (0.018 g, 0.027 mmol) was dissolved in ethylene glycol (3 mL) and this was added to the mixture. The reaction was then left to reflux for 4 days. The mixture was then allowed to cool and the black AgCl was removed by centrifugation, after which the remaining solution was reduced under vacuum to 3 mL. Water (5 mL) and a few drops of a concentrated NH_4PF_6 solution were then added. The resulting dark precipitate was collected and washed with water and diethyl ether (25 mL each). The product was then recrystallized from acetone/water (2:1, 20 mL). On HPLC[8a] no bpt monomer was detected. Due to its high charge the product did not elute from the column. Yield: 80%. Anal. Found (calcd): C, 35.9 (35.5); H, 2.6 (2.5); N, 11.1 (11.5).

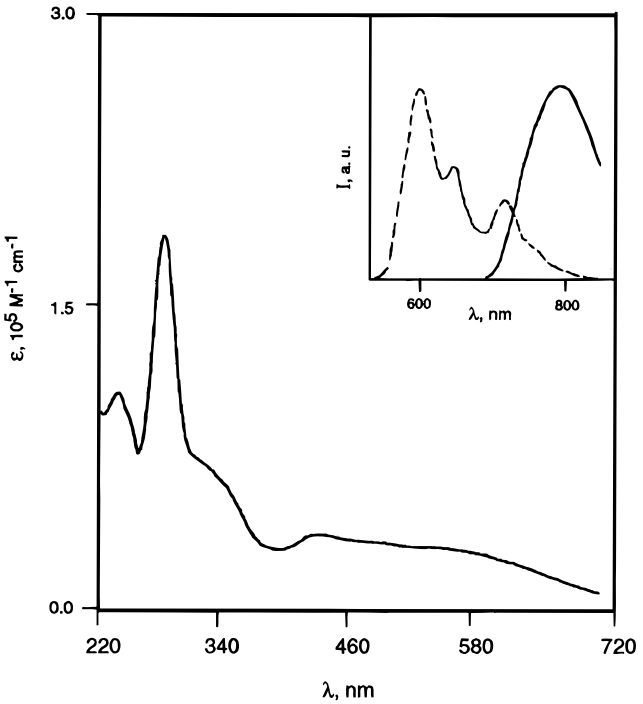

Figure 2. Absorption spectrum in acetonitrile solution and (inset) luminescence spectra of **1** (solid line, room-temperature acetonitrile solution; dashed line, 77 K MeOH/EtOH 4:1 rigid matrix, $\lambda_{exc} = 400$ nm).

Results

Synthesis of **1** was performed by taking advantage from the well-known *complexes as ligands and complexes as metals* synthetic strategy.[2] In particular, $[Ru(bpy_2(bpt)]^+$ was used as the complex-ligand species, and as the complex-metal partner $[Cl_2Ru(\mu\text{-2,3-dpp})Ru(bpy)_2\}_2]^{4+}$ was employed, in a 1:1 ratio.

The new compound is stable in solution under the experimental conditions used for at least a couple of weeks, as demonstrated by the stability of its absorption spectrum. The electronic spectrum in acetonitrile solution (Figure 2) shows an intense feature in the UV region ($\lambda_{max} = 285$ nm, $\epsilon = 156\,500$ M^{-1} cm^{-1}) and a moderately intense and broad absorption in the visible region ($\lambda_{max} = 435$ nm, $\epsilon = 36\,600$ M^{-1} cm^{-1}; $\lambda_{max} = 535$ nm, $\epsilon = 27\,000$ M^{-1} cm^{-1}).

(6) (a) Haga, M.; Ano, T.; Kano, K.; Yamabe, S. *Inorg. Chem.* **1991**, *30*, 3843. (b) Onho, T.; Nozaki, K.; Haga, M. *Inorg. Chem.* **1992**, *31*, 4256. (c) Nozaki, K.; Ohno, T.; Haga, M. *J. Phys. Chem.* **1992**, *96*, 10880.
(7) (a) Lei, Y.; Buranda, T.; Endicott, J. F. *J. Am. Chem. Soc.* **1990**, *112*, 8820.(b) Beley, M.; Collin, J.-P.; Louis, R.; Metz, B.; Sauvage, J.-P. *J. Am. Chem. Soc.* **1991**, *113*, 8521. (c) Beley, M.; Chodorowski-Kimmes, S.; Collin, J.-P.; Lainé, P.; Launay, J.-P.; Sauvage, J.-P. *Angew. Chem., Int. Ed. Engl.* **1994**, *33*, 1775.
(8) (a) Hage, R.; Dijkhuis, A. H. J.; Haasnoot, J. G.; Prins, R.; Reedijk, J.; Buchanan, B. E.; Vos, J. G. *Inorg. Chem.*, **1988**, *27*, 2185. (b) Barigelletti, F.; De Cola, L.; Balzani, V.; Hage, R.; Haasnoot, J. G.; Reedijk, J.; Vos, J. G. *Inorg. Chem.* **1989**, *28*, 4344. (c) De Cola, L.; Barigelletti, F.; Balzani, V.; Hage, R.; Haasnoot, J. G.; Reedijk, J.; Vos, J. G. *Chem. Phys Lett.* **1991**, *178*, 491. (d) van Diemen, J. H.; Hage, R.; Haasnoot, J. G.; Lempers, H. E. B.; Reedijk, J.; Vos, J. G.; De Cola, L.; Barigelletti, F.; Balzani, V. *Inorg. Chem.* **1992**, *31*, 3518. (e) Hage, R.; Haasnoot, J. G.; Reedijk, J.; Vos, J. G. *Chemtracts, Inorg. Chem.* **1992**, *4*, 75. (f) Hage, R., PhD Thesis, University of Leiden, The Netherlands, 1988.
(9) Giuffrida, G.; Campagna, S. *Coord. Chem. Rev.* **1994**, *135*−136, 517.
(10) (a) Juris, A.; Balzani, V.; Barigelletti, F.; Campagna, S.; Belser, P.; von Zelewsky, A. *Coord. Chem. Rev.* **1988**, *84*, 85; (b) Kalyanasundaram, K. *Photochemistry of Polypyridine and Porphyrin Complexes*; Academic Press: London, 1991.
(11) (a) De Armond, M. K.; Carlin, C. M. *Coord. Chem. Rev.* **1981**, *36*, 325. (b) Meyer, T. J. *Pure Appl. Chem.* **1986**, *58*, 1193.

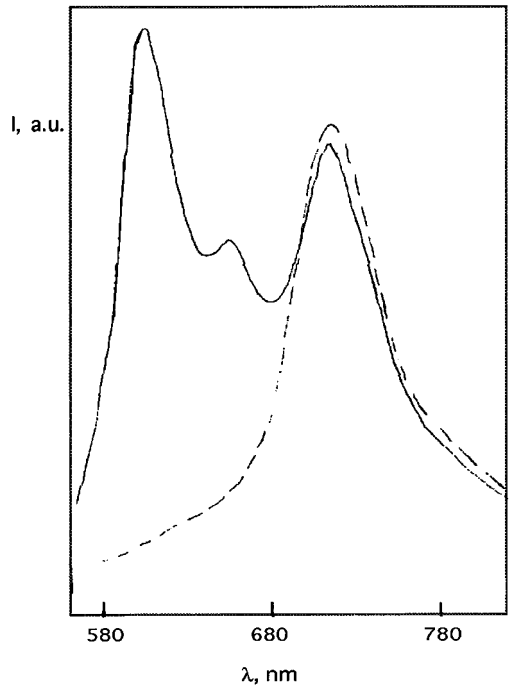

Figure 3. Emission spectra of **1** in MeOH/EtOH 4:1 (v/v) rigid matrix at 77 K: solid line, excitation wavelength 420 nm; dashed line, excitation wavelength 530 nm.

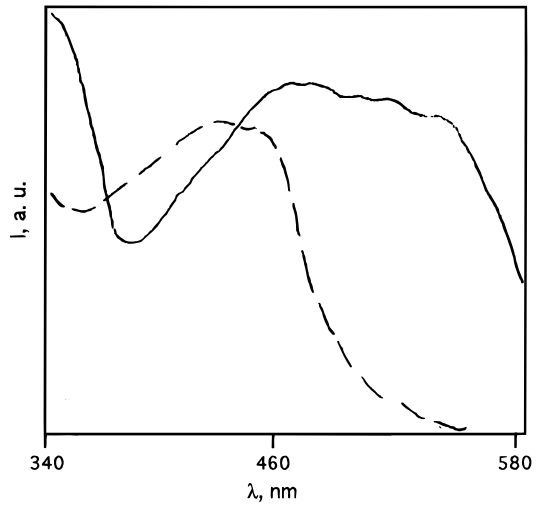

Figure 4. Corrected excitation spectra of **1** in MeOH/EtOH 4:1 (v/v) rigid matrix at 77 K: solid line, emission wavelength 720 nm; dashed line, emission wavelength 600 nm.

At room temperature in fluid solution complex **1** exhibits only one emission feature, with a strictly monoexponential lifetime. The excitation spectrum, recorded at the emission maximum, closely overlaps the absorption spectrum in the region 360−740 nm (for technical reasons we were unable to obtain a reliable excitation spectrum at shorter wavelength). At 77 K in rigid glass **1** exhibits two independent emissions, which show excitation wavelength dependence: when the excitation wavelength is 420 nm, the emission spectrum peaks at 600 nm, with a lower intensity component at 720 nm. When the excitation wavelength is 530 nm, the emission spectrum peaks at 720 nm, and the higher energy component is negligible. Accordingly, excitation spectra measured at 600 nm and 720 nm are different each other. The luminescence spectra obtained upon excitation at 400 nm at room temperature and at 77 K are shown in the inset of Figure 2. Figure 3 shows emission spectra at 77 K recorded with two different excitation wavelengths. Figure 4 shows 77 K corrected excitation spectra performed at two diffent emission wavelengths. Spectroscopic and photophysical data are listed in Table 1.

Cyclic and differential pulse voltammetry showed that the new complex **1** undergoes several redox processes in the potential window examined (+1.80/−2.00 V *vs* SCE). The potential values and the number of electrons exchanged for each wave are given in Table 2.

Spectroelectrochemical oxidation of **1** was performed at 1.05 V *vs* Ag/AgCl in acetonitrile solution at room temperature. Concentration of the complex in a typical experiment was about 5×10^{-4} M, 0.1 M TEAP was used as supporting electrolyte, and a few drops of 6% HNO_3 were added to stabilize Ru(III) metal ion. Spectroscopic changes upon oxidation are shown in Figure 5.

Discussion

Redox Behavior. Oxidation and reduction processes of Ru(II)−polypyridine complexes are known to be metal-centered and ligand-centered, respectively.[10,11] In the multicomponent species **1** studied here, there are three different types of metals (see Figure 1): the central metal, which is connected to three bridges (Ru_C); the two Ru(II) of the (μ-2,3-dpp)Ru(bpy)$_2^{2+}$ subunits (Ru_B); the Ru metal, which is connected to two terminal bpy ligands and to the anionic bridge (Ru_A). By comparison with literature values (see also Table 2), the Ru(II) metal of the (μ-bpt)Ru(bpy)$_2^+$ subunit (Ru_A)[8a] is expected to be oxidized at a less positive potential than the two (μ-2,3-dpp)Ru(bpy)$_2^{2+}$ moieties (Ru_B),[4] which in their turn should be oxidized at a less positive potential than the central Ru(II) metal (Ru_C).[4] As far as the polypyridine ligands are concerned, reduction potentials should shift to more negative values in the series μ-2,3-dpp, bpy, μ-bpt.[4,8]

The oxidation pattern of **1** exhibits two reversible oxidation waves, with $E_{1/2}$ at +1.09 and +1.55 V, respectively (Table 2). The intensity of the wave at more positive potential is twice that of the other one. On the basis of the above considerations, the first wave is attributed to oxidation of Ru_A, and the second wave is assigned to simultaneous one-electron oxidation of both the Ru_B metals. Oxidation of the central Ru_C metal is expected out of the potential window investigated.[4] The oxidation of the (bpy)$_2$Ru(μ-dpt)$^+$ subunit in **1** is slightly shifted to more positive potentials with respect to oxidation of the corresponding subunit in **3** (+1.09 *vs* +1.04). Such a shift is justified by considering the different electron withdrawing properties of the [(bpy)$_2$Ru(μ-2,3-dpp)]Ru^{6+} and (bpy)$_2$Ru^{2+} subunits which coordinate the (μ-dpt)Ru(bpy)$_2^+$ moiety in **1** and **3**, respectively.

On reduction, two reversible single electron waves are observed at −0.64 and −0.89 V, followed by two other overlapping and poorly resolved waves, which concern a larger number of electrons (four electrons for each wave, from DPV analysis[4b]). The first two processes are assigned to the one-electron reduction of the two (interacting) μ-2,3-dpp bridges, the third wave is attributed to the one-electron reduction of a bpy for each terminal Ru moiety, and the fourth process should concern the first reduction of the second bpy of each terminal moiety. Most likely, the third and the fourth waves also comprise the successive second reductions of the μ-2,3-dpp bridges.[12] Actually, the second reduction of μ-2,3-dpp is known to occur at similar (or even slightly less negative) potential than first reduction of bpy in multinuclear metal complexes.[4a] The presence of an electron-rich (donor) anionic bridge in the coordination sphere of the central metal moves the μ-2,3-dpp ligands reductions to more negative potentials in **1** with respect to the corresponding reductions in **2** (Table 2). This effect is

(12) As expected, the third and the fourth reduction waves have $E_c - E_a$ values significantly larger than 60 mV.

Table 1. Absorption and Emission Data[a]

complex		abs (298 K) λ_{max}, nm	luminescence (298 K)			luminescence (77 K)	
no.	formula	(ϵ, M^{-1} cm^{-1})[b]	λ_{max}, nm[c]	τ, ns	Φ	λ_{max}, nm[c]	τ, μs
1	$[(bpy)_2Ru(bpt)Ru\{(dpp)Ru(bpy)_2\}_2]^{7+}$	535 (27 000)	800	68	0.001	600	4.0[d]
						720	1.6[e]
2	$[Ru\{(dpp)Ru(bpy)_2\}_3]^{8+}$ [f]	540 (45 000)	802	70	0.001	727	1.4
3	$[(bpy)_2Ru(bpt)Ru(bpy)_2]^{3+}$ [g]	453 (18 500)	648	100	0.002	608	3.6

[a] Data are in acetonitrile deareated solution (298 K) or in MeOH/EtOH 4:1 rigid matrix (77 K). Typical concentration of the compounds are in the range 1×10^{-5} to 1×10^{-4} M. [b] Lowest energy absorption maximum. [c] Luminescence maxima are corrected for photomultiplier response. [d] Lifetime measured at 580 nm; $\lambda_{exc} = 337$ nm. [e] Lifetime measured at 760 nm; $\lambda_{exc} = 337$ nm. [f] Data from ref 4a,g. [g] From ref 8a.

Table 2. Electrochemical Data[a]

	oxidn	redn
1	+1.09 [1] (Ru_A); +1.55 [2] (Ru_B)[b]	−0.64 [1]; −0.89 [1]; −1.49 [∼4];[c] −1.75 [∼4][c]
2[d]	+1.53 [3]	−0.62 [1]; −0.77 [1]; −1.23 [1]
3[e]	+1.04 [1]; +1.34 [1]	−1.40 [2]; −1.62 [1]; −1.67 [1]

[a] $E_{1/2}$ values in acetonitrile. Potentials *vs* SCE. Working electrode: glassy carbon electrode. The figures in brackets refer to the number of electrons exchanged. All the redox processes are reversible unless otherwise stated. Typical compounds concentration, 5×10^{-4} M. [b] Oxidation assignments are reported in parentheses. Metal atoms are indicated as in Figure 1. [c] Quasi-reversible process; the potential refers to anodic peak. [d] Data from ref 4a,g. [e] From ref 8a.

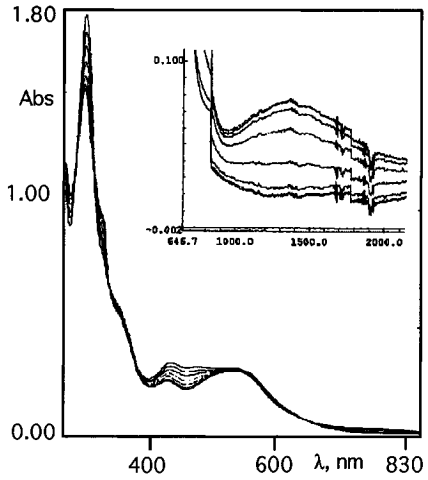

Figure 5. Spectroscopic changes on electrochemical oxidation of **1**: oxidation potential, 1.05 V *vs* Ag/AgCl; supporting electrolyte, 0.1 M TEAP; solvent, acetonitrile. A few drops of 6% HNO_3 were added to stabilize the Ru(III) metal-based component. Scans were taken at regular intervals over a period of 30 min.

more important for the second μ-2,3-dpp than for the first one (compare −0.64 *vs* −0.62 V for the first reduction in **1** and **2**, respectively, with −0.77 and −0.89 V for the second reduction, Table 1). The reason is that the second reduction in **1** cannot be stabilized by electron delocalization upon the other, already negatively-charged, bridges, contrary to what happens for the second reduction of **2**.[13]

Absorption Spectrum, Luminescence Properties, and Intercomponent Transfer Processes. The UV region of the absorption spectrum of **1** is dominated by the strong ligand-centered (LC) transitions of the bpy ligands, which are known

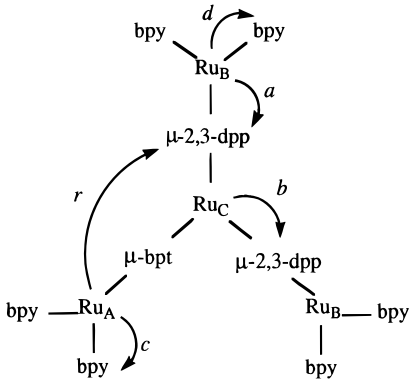

Figure 6. Lowest energy electronic transitions occurring in **1** (only transitions relevant to the discussion are represented; *r* is the "remote" transition reported in the text).

to be found at about 280 nm.[10] The 2,3-dpp-centered transitions essentially contribute to the shoulder around 340 nm (Figure 2).

Because of the multicomponent nature of the complex, a number of different metal-to-ligand charge transfer (MLCT) bands are expected, such as transitions *a*, *b*, *c*, and *d* (leaving aside higher energy transitions involving the anionic bridge and "remote" CT transitions, such as *r*) represented in Figure 6. On the basis of the electrochemical data, the energies of such transitions should increase in the series $a < b \leq c < d$ (the energy order for the relative energies of *b* and *c* is uncertain). This situation explains the very broad absorption feature of the compound, which extends all throughout the visible region. Owing to the very broad absorption feature and the relatively high number of transitions involved, spectral fitting of the visible region failed to give reliable results. In our case, in fact, *at least* two different best fittings (both of them apparently satisfactory ones, see Supporting Information, Figure S1) could be obtained, in which contribution from five bands is considered to simulate the experimental visible spectrum. Whereas the number of the bands needed is constant in the various spectral fittings obtained, their energy positions and relative intensities are significantly different. The only useful information which can be obtained from best fitting analysis is the presence of a low energy broad band (ϵ_{max} about 4000 M^{-1} cm^{-1}, half-width about 1500 cm^{-1}) centered in the range 640 - 660 nm, which could be assigned to the remote CT transitions *r* showed in Figure 6. The strong uncertainties on the spectral fittings limit further discussion of this band.

The luminescence of **1** at room temperature in fluid solution is quite similar to that of the parent compound **2** (Table 1), indicating the same luminescent level for both compounds, that is the $(bpy)_2Ru\rightarrow\mu$-2,3-dpp (i.e.; $Ru_B\rightarrow\mu$-2,3-dpp) CT excited state.[4] The slight blue-shift of the emission on going from **2** to **1** (Table 1) can be explained by taking into account the different reduction potentials of bridged dpp in the two complexes, as discussed above.

The similarity in the visible region of the excitation and absorption spectra of **1** in acetonitrile fluid solution at room

(13) First and second reductions of a tris-chelate metal complex containing ligands with low-lying π^* orbitals are stabilized by ligand−ligand interactions mediated through the metal, while the third reduction can be destabilized by the same interactions (for further details on this point, see ref 14). While the second reduction of **2** can be stabilized by the presence of the third, unreduced, μ-dpp, the corresponding reduction in **1** cannot take advantage of the presence of ligands with empy, low-lying π^* orbitals in the coordination sphere of the central metal.

(14) Serroni, S.; Juris, A.; Campagna, S.; Venturi, M.; Denti, G.; Balzani, V. *J. Am. Chem. Soc.* **1994**, *116*, 9086.

temperature demonstrates that at this temperature efficient intercomponent energy transfer occurs from the upper-lying (μ-bpt)(bpy)Ru→bpy (i.e.; Ru_A→bpy) CT excited state of the $Ru(bpy)_2(\mu\text{-bpt})^+$ component to the lower-lying Ru_B→μ-2,3-dpp CT excited state of the $Ru(bpy)_2(\mu\text{-2,3-dpp})^{2+}$ subunit(s) (the driving force of the process, ΔG, is -0.34 eV).[15]

Intercomponent energy transfer appears to be less efficient at 77 K in rigid matrix, where two emissions with essentially the typical lifetimes of $*(bpy)_2Ru(\mu\text{-bpt})^+$ and $*(bpy)_2Ru(\mu\text{-2,3-dpp})^{2+}$ components are found (Table 1), thus suggesting that $(bpy)_2Ru(\mu\text{-bpt})^+$ and $(bpy)_2Ru(\mu\text{-2,3-dpp})^{2+}$ components can be regarded as "isolated" components of the supermolecule **1** at 77 K. This is furthermore supported by considering the low temperature excitation and emission spectra (Figures 3 and 4): from emission spectra performed at different excitation wavelength, one can note (Figure 3) that excitation in the 420-460 nm region (the region in which the absorption of the Ru_A-based chromophore is relatively more important[8]) yields an emission spectrum dominated by Ru_A→bpy CT emission (the emission maximum at about 650 nm is due to the typical vibrational progression of the Ru→bpy CT emission band at 77 K[10]), while 530 nm excitation (i.e. in the absorption bands due to the Ru_B-based chromophores[4]) yields the typical emission of the peripheral $(bpy)_2Ru(\mu\text{-2,3-dpp})^{2+}$ components.[8] On the other hand, it is clear from Figure 4 that the Ru_A-based chromophore is responsible for the high energy emission, and the Ru_B-based chromophores are responsible for the lower energy emission. It should also be noted that the corrected excitation spectra of **1** (visible maximum at 430 nm, Figure 4) is significantly different from that of the parent mononuclear complex $[Ru(bpy)_2(bpt)]^+$ (maximum at 453 nm in MeOH/EtOH 1:4)[8f] and from that of the closely related dinuclear complex $[(bpy)_2Ru(bpt)Ru(bpy)_2(bpt)]^{3+}$ (maximum at 475 nm in MeOH/EtOH 1:4),[8f] thus definitively excluding the hypothesis of the presence of these species as the origin of the high-energy emission.

Luminescence lifetimes measured at 580 and at 760 nm (excitation wavelength 337 nm in both cases) yield monoexponential decays of 4.0 and 1.6 μs, respectively, typical of "isolated" Ru→bpy CT and of Ru→μ−2,3-dpp CT excited states (Table 1). The spectral separation between the two emissions evidently permits spectral resolution of lifetimes. Time-resolved emission spectra (Supporting Information, Figure S2) confirm the attribution of the emission bands (see above), showing that the high-energy emission is the longer-lived one.

The 77 K results are quite surprising on considering that intercomponent energy transfer is efficient even at 77 K in parent complexes such as $[(bpy)_2Ru(\mu\text{-bpt})Os(bpy)_2]^{3+}$ (**4**)[8c] and $[(bpy)_2Ru(\mu\text{-2,5-dpp})Ru\{\mu\text{-2,3-dpp})Ru(bpy)_2\}_2]^{8+}$.[16] In particular, the Ru→bpy CT excited state is totally quenched in **4** by energy transfer with sensitization of the Os→bpy CT level, at both room temperature and 77 K.[8c]

We propose that the different behavior of **1** and **4** as far as the temperature dependence of the energy transfer is concerned can be explained when detailed mechanisms for energy transfer are taken into account. Intercomponent energy transfer in multinuclear metal complexes can occur by an electron exchange (Dexter) mechanism;[17] however, in many cases the boundaries between energy and electron transfer processes in polynuclear metal complexes are ambiguous,[4af,18,19] and energy transfer can be efficiently mediated by electron transfer steps.[4a,18,19] In the case of **4**, electron transfer from $(bpy)_2Os(\mu\text{-bpt})^+$ subunit to the excited Ru-based component (Figure 7, process *I*) could be the first step of a two-step mechanism which would speed the overall Ru→bpy to Os→bpy energy transfer process.[20] Process *I* is expected to be fast (there is a good communication between the metals,[8c] e.g. high electronic coupling; furthermore, the reorganization energy should be relatively low because of the short distance of the electron transfer). Because of the large electronic coupling and the small reorganization energy, this mechanism is also expected to be efficient at 77 K.

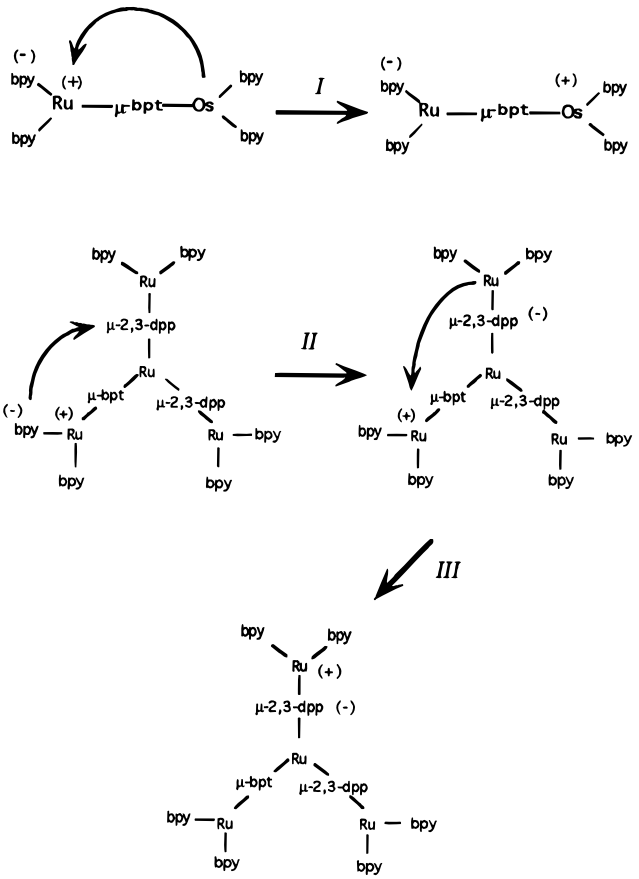

Figure 7. Electron transfer processes which are proposed to be involved in **4** and **1** to mediate intercomponent energy transfer processes (see text).

In **1**, the analogous reductive electron transfer process is forbidden for energetic reasons. However, a two-step energy transfer could occur by oxidative electron transfer from a $*(bpy)_2Ru(\mu\text{-bpt})^+$ subunit to a $(\mu-2,3\text{-dpp})Ru(bpy)_2^{2+}$ component (Figure 7, process *II*), with production of a "remote" CT level (this level corresponds to transition *r* in Figure 6). Process *II* is esoergonic by 0.34 eV[21] and could drive the overall process. In fact, the "remote" CT level would undergo to a second electron transfer (Figure 7, process *III*) to ultimately yield the luminescent triplet $*(bpy)_2Ru(\mu-2,3\text{-dpp})^{2+}$ excited state. Electronic coupling for the long-range electron transfer *II* should be much lower than for *I*. Furthermore, the reorganization energy (which depends on the distance of the electron transfer[22]) would also expected to be much higher. Higher reorganization

(15) The driving force of the process was calculated from the E_{00} values of the two emissions of **1** at low temperature.
(16) Denti, G.; Serroni, S.; Campagna, S.; Ricevuto, V.; Balzani, V. *Inorg. Chim. Acta* **1991**, *182*, 127.
(17) Dexter, D. L. *J. Chem. Phys.* **1953**, *21*, 836.
(18) Tapolsky, G.; Deusing, R.; Meyer, T. J. *J. Phys. Chem.* **1989**, *93*, 3885.
(19) Giuffrida, G.; Calogero, G.; Ricevuto, V.; Campagna, S. *Inorg. Chem.* **1995**, *34*, 1957.
(20) Note that the charge-separated state produced by step *I* of Figure 7 would convert very rapidly into the Os→bpy CT level by a second electron transfer.
(21) The driving force ΔG of the process was calculated as follows: $\Delta G = *E_{ox} - E_{red}$, where $*E_{ox}$ is the excited state oxidation energy of the donor unit ($*E_{ox} = E_{ox} - E_{00}$) and E_{red} is the reduction energy of μ-2,3-dpp. E_{00} is the excited state energy of the $(bpy)_2Ru(\mu\text{-bpt})^+$ component.

energies produce larger temperature and medium effects on the efficiency of electron transfer processes.[23] The low electronic coupling and the high reorganization energy of the first electron transfer step of the two-step energy transfer mechanism in **1** would translate in a high nuclear barrier and could explain the inefficiency of the intercomponent transfer process in rigid matrix at 77 K.

In order for the two-step mechanism to operate, electron transfer from the "remote" CT level to produce $*(bpy)_2Ru(\mu\text{-}2,3\text{-}dpp)^{2+}$ (process *III* in Figure 7) should be relatively fast, in spite of the fact that this process is almost isoergonic:[24] actually, a hole-transfer superexchange mechanism involving the anionic bpt bridge, the central Ru metal, and the *reduced* 2,3-dpp bridge (i.e.; another anionic bridge) is expected to yield a strong long-distance metal−metal communication between the oxidized Ru(III) of the $(bpy)_2Ru(\mu\text{-bpt})$ component and the donor Ru(II) metal of the reduced $(\mu\text{-}2,3\text{-dpp})Ru(bpy)_2^{+}$ unit.[9] Anionic bridging ligands are indeed known to promote strong metal−metal interactions in multicomponent systems.[5−7,25] The presence of the anionic bridge would therefore be decisive to obtain such a strong communication and speed up the second electron transfer step.[26] Furthermore, competitive direct charge recombination from the remote CT level to the ground state should probably lie in the Marcus inverted region ($\Delta G \sim 1.73$ eV[24]) and is expected to be not very fast.

Spectroelectrochemical Oxidation. Because of the high number of redox sites which are present in **1** and in similar multicomponent compounds, spectroelectrochemical investigations on these species are quite interesting and can provide useful information on the contribution of the various MLCT transitions to the visible absorption and on the extent of the electronic interaction between the metal-based chromophores. As the first step toward this direction, here we will discuss the spectrum of the singly oxidized form of the title compound.

Spectroelectrochemical oxidation of **1** was performed at 1.05 V *vs* Ag/AgCl in acetonitrile at room temperature. At this potential, only oxidation of Ru_A occurs (see redox section). Clean isosbestic points at about 640, 330, 300, and 280 nm were maintained during the course of the oxidation process (Figure 5). On reduction back to 0 V, the initial spectrum is almost totally recovered, showing the reversibility of the process. The main spectral changes (Figure 5) can be interpreted as follows. (i) The decrease of the absorption in the region around 430 nm is mainly due to the disappearing of the $Ru_A \rightarrow$bpy CT transitions (transition *c* in Figure 6) and, at a minor extent, of the $Ru_A \rightarrow \mu$-bpt CT transition, expected in the region 330−400 nm.[8] (ii) The decrease of the bpy-centered absorption peaking at ∼285 nm with the contemporary increase of the absorption in the region 300−330 nm is due to the red-shift of the ligand-centered transition involving the two bpy ligands coordinated to Ru_A. Actually, bpy-centered transitions in $[Ru(bpy)_3]^{3+}$ occur at lower energies than the corresponding transitions in $[Ru(bpy)_3]^{2+}$.[10] (iii) Increased absorption at $\lambda > 660$ nm is probably due to LMCT transitions (i.e.; μ-bpt$\rightarrow Ru_A^{III}$ CT).

Interestingly, even an infrared absorption band appears ($\lambda_{max} = 1370$ nm; $\epsilon_{max} = 1870$ M^{-1} cm^{-1}; half-width = 3690 cm^{-1}; Figure 5, inset), which can be assigned to an intervalence transfer transition ($Ru_C^{II} \rightarrow Ru_A^{III}$ CT). By using the common Hush equation[29] to calculate the electronic delocalization coefficient α^2 between the redox centers Ru_C and Ru_A, a value of 0.010 is obtained (the Ru_C-Ru_A distance is assumed to be 6.18 Å). The fact that the α^2 value is much smaller than the unity confirms the supramolecular nature of **1**, in that the valencies can be considered trapped.[30]

Conclusion

The first polynuclear luminescent and redox-active compound (**1**) in which both electron-rich and electron-poor polypyridine bridging ligands are present has been prepared, and its spectroscopic, photophysical, and electrochemical properties have been studied and compared with those of parent complexes. Excited states and oxidation and reduction processes are localized in specific sites of the multicomponent structure. However, perturbations of each component on the redox and excited states of the other subunits of the multinuclear system can be evidenced, as well as electronic interactions between the metal-based components. Intercomponent energy transfer is efficient in **1** in fluid solution at room temperature, whereas the process is not observed in rigid matrix at 77 K. An energy transfer mechanism mediated by two successive electron-transfer processes has been proposed to rationalize the photophysical properties.

Acknowledgment. We thank Prof. V. Balzani and Dr. F. Barigelletti for helpful discussions. This work was supported by the Ministero della Ricerca Scientifica e Tecnologica, by the CNR, and by Forbairt. S.S. also thanks the CNR for Grant No. 201.03.20.

Supporting Information Available: Figures S1 and S2, showing spectral fitting of the absorption spectrum of **1** in the visible region and time-resolved emission spectra of **1** in rigid matrix at 77 K, respectively (3 pages). Ordering information is given on any current masthead page.

IC950086A

(22) (a) Marcus, R. A. *Discuss. Faraday Soc.* **1960**, *29*, 21. (b) Marcus, R. A.; Sutin, N. *Biochim. Biophys. Acta* **1985**, *811*, 265.
(23) See, for example: Verhoeven, J. W.; Paddon-Row, M. N.; Warman, J. M. In *Photoprocesses in Transition Metal Complexes, Biosystems and Other Molecules: Experiment and Theory*; Kochanski, E., Ed.; Kluwer: Dordrecht, The Netherlands, 1992; p 233.
(24) The energy of the $*(bpy)_2Ru(\mu-2,3\text{-}dpp)^{2+}$ subunit is 1.72 eV (obtained from the E_{00} energy at 77 K, see also ref 15), and the energy of the "remote" CT level is estimated to be ∼1.73 eV (obtained from the excited state energy of the bpt-containing peripheral subunit, 2.07 eV, decreased by 0.34 eV (see ref 21). Note that this is not reflected by the redox properties of the Ru(II) atoms. Coulombic stabilization of the electron-hole pair in $*(bpy)_2Ru(\mu-2,3\text{-}dpp)^{2+}$ balances the different oxidation potentials of the metal ions.
(25) (a) Bignozzi, C. A.; Paradisi, C.; Roffia, S.; Scandola, F. *Inorg. Chem.* **1988**, *37*, 408. (b) Haga, M.; Bond, M. A. *Inorg. Chem.* **1991**, *30*, 475. (c) Endicott, J. F.; Song, X.; Watzsky, M. A.; Buranda, T.; Lei, Y. *Chem. Phys.* **1993**, *176*, 427.
(26) It should be considered that a possible mechanism for intercomponent energy transfer is also Förster mechanism.[27] From the data in Table 1, by considering the overlap between the donor emission and the acceptor absorption, and estimating a donor−acceptor distance of 13 Å (approximately the distance between the metal centers of the $(bpy)_2Ru(\mu\text{-bpt})^{+}$ and $(bpy)_2Ru(\mu\text{-}2,3\text{-dpp})^{2+}$ subunits), a 100% efficiency for the Förster energy transfer is obtained, even at 77 K, by using the common equations for dipole−dipole energy transfer.[28] The disagreement between calculation and experimental results seems to suggest that the usual approximations employed in calculating Förster energy transfer for isolated molecules (statistical terms are used for taking into account the mutual orientation of donor and acceptor electric dipoles) could not be suitable for calculating Förster energy transfer efficiency in supermolecules in which rigid orientations of the interacting dipoles are present.
(27) Förster, Th. *Discuss. Faraday Soc.* **1959**, *27*, 7.
(28) See, for example: Gilbert, A.; Baggott, J. *Essentials of Molecular Photochemistry*; Blackwell, Oxford, U.K., 1991; Section 5.3.
(29) Hush, N. S. *Electrochim. Acta* **1968**, *13*, 1005.
(30) Vogler, A. In *Photoinduced Electron Transfer* , Fox, M. A.; Chanon, M. (Eds.), Elsevier, 1988, Part D, p. 179.